JOURNAL OF CATALYSIS

Structural requirements and reaction pathways in methane activation and chemical conversion catalyzed by rhodium

Junmei Wei and Enrique Iglesia [*]

Department of Chemical Engineering, University of California at Berkeley, Berkeley, CA 94720, USA

Abstract

Kinetic and isotopic tracer methods led to a simple and unifying mechanistic proposal for reactions of CH_4 with CO_2 and H_2O, for its decomposition on Rh clusters, and for water–gas shift reactions. Kinetic rates for forward reactions were measured by correcting net rates for approach to equilibrium and by eliminating transport artifacts. These rates were proportional to CH_4 pressure (5–450 kPa) and independent of CO_2 or H_2O pressures (5–450 kPa) on all supported Rh catalysts; the resulting first-order rate constants were identical for H_2O and CO_2 reforming and for CH_4 decomposition. Kinetic isotope effects ($k_{CH_4}/k_{CD_4} = 1.54$–1.60) were also independent of the concentration or identity of the co-reactant, consistent with the sole kinetic relevance of C–H bond activation steps. These data indicate that co-reactant activation and its kinetic coupling with CH_4 activation via scavenging of chemisorbed carbon intermediates are fast steps and lead to Rh surfaces essentially uncovered by reactive intermediates during H_2O and CO_2 reforming. CO oxidation rates before and after reforming reactions showed that Rh surfaces remain uncovered by unreactive species during reforming catalysis under conditions relevant to industrial practice. CH_4 conversion rates for $CH_4/CD_4/CO_2$ reactant mixtures are much faster than $CH_{4-x}D_x$ formation rates, indicating that C–H bond activation elementary steps are irreversible. $CH_4/CO_2/D_2$ reactant mixtures led to binomial isotopomer distributions in dihydrogen and water at all reactant conversions. Their D contents were identical and corresponded to equilibration between all H atoms in reacted CH_4 and all D_2 in the inlet stream. Thus, recombinative desorption steps of H atoms and OH groups to form H_2 or H_2O are quasi-equilibrated during CH_4 reforming. $^{12}CH_4/^{12}CO_2/^{13}CO$ mixtures led to identical ^{13}C contents in CO and CO_2, as expected from quasi-equilibrated CO_2 activation steps. The quasi-equilibrated nature of all these steps requires that water–gas shift reactions also be at equilibrium during CH_4 reforming, as found experimentally. CH_4 reforming turnover rates increased as the size of Rh clusters supported on Al_2O_3 or ZrO_2 decreased, suggesting that coordinatively unsaturated Rh surface atoms prevalent in smaller clusters activate C–H bonds more effectively than atoms on lower-index surfaces, as also found on single-crystal surfaces. Turnover rates do not depend on the identity of the support; any involvement of the support in the activation of co-reactants is not kinetically relevant.
© 2004 Elsevier Inc. All rights reserved.

Keywords: CH_4 activation; CH_4 reforming; Rh catalysts; Isotopic tracer; Kinetic isotope effects; Cluster size effects

1. Introduction

CH_4 reforming with CO_2 or H_2O provides an effective route to synthesis gas streams useful as precursors to fuels and petrochemicals. Several hundred studies have documented scientific and technological progress over the past few years, including reviews by Edwards and Maitra [1], Wang and Lu [2], and Bradford and Vannice [3]. After the initial report by Fischer and Tropsch [4] that group VIII metals (Ni, Ru, Rh, Pt, Pd, Ir) catalyze CO_2–CH_4 reactions,

active debate continues about the relative intrinsic reactivities of different metals, while Rh is generally considered to be one of the most stable group VIII metals [5–10]. Rh/Al_2O_3 [6–18], Rh/ZrO_2 [11,17], Rh/SiO_2 [11,13,17, 19–21], Rh/MgO [9,13,14,17,22], Rh/La_2O_3 [13,14,17,21], Rh/TiO_2 [13,14,17,23,24], Rh/NaY [25], and Rh/ZSM-5 [26] have also been shown to catalyze CO_2 and H_2O reforming of CH_4.

Rigorous and unequivocal assessments of relevant elementary steps and of dispersion and support effects on turnover rates remain unavailable, and many contradictory proposals and findings are still unresolved, even after significant research efforts. A qualitative theoretical analysis based

on bond-order bond-energy conservation led to the suggestion that both CH_4 and CO_2 dissociation steps are kinetically relevant on Rh(111) [27]. Rostrup-Nielsen and Bak Hansen [5] reported that H_2O reforming rates are much faster than reforming CO_2 rates and that the latter depended on rate-determining CO_2 activation steps on Rh/Al_2O_3. Studies of the stoichiometric activation of CO_2 and CH_4 on Rh/Al_2O_3 led to the conclusion that both CH_4 and CO_2 limit overall rates, and first-order rate dependencies on CO_2 and CH_4 were proposed [28]. Using phenomenological power law kinetics of the form

$$r = k P_{CH_4}^a P_{CO_2}^b, \qquad (1)$$

Bhat and Sachtler [25] reported that the CO_2 reforming of CH_4 is first-order in CH_4 and zero-order in CO_2 on Rh/NaY catalyst, indicating that C–H bond activation is the kinetically relevant step in CH_4 reforming reactions and hydrogen desorption to form H_2 and that CO_2 reactions with CH_4-derived chemisorbed species to form CO are fast and kinetically- invisible, in agreement with our recent findings on Ru-based catalysts [29].

Many studies on model metal surfaces have suggested that C–H bond activation is the kinetically relevant step in CH_4 conversion to H_2–CO mixtures [30, and references therein]. C–H bond dissociation occurs faster on step and kink sites than on terrace sites, apparently as a result of the greater coordinative unsaturation of surface metal atoms on rough surfaces [31–33]. When this step limits overall chemical conversion rates, its strong structure sensitivity, by the definition of Boudart [34], is expected to cause significant effects of metal dispersion and cluster size on catalytic turnover rates. Computational studies using density functional theory suggested that steps and kinks decrease CH_4 dissociation barriers [33]. These barriers are estimated to be about 30 kJ/mol lower on steps and kinks present on Rh(211) surfaces than on close-packed terrace planes on Rh(111) [33]. Wang and Ruckenstein [17] reported that CO_2 reforming is structure-sensitive on Rh/Al_2O_3; the turnover rates depend significantly on Rh crystallite size (1–7 nm) and the specific activity increased with increasing Rh dispersion on Rh/Al_2O_3 catalysts, but most data were measured near equilibrium without appropriate correction. Zhang et al. [13] have reported similar dispersion effects for CO_2 reforming of CH_4 on Rh/Al_2O_3. The effects of Rh dispersion on CH_4–H_2O reactions have not been reported.

Supports are often claimed to influence CH_4 reforming rates on Rh crystallites, but their concomitant effects on Rh dispersion or on ubiquitous transport artifacts are seldom rigorously excluded, and significant discrepancies exist among these previous reports. Wang and Ruckenstein [17] reported that CO_2 reforming rates on Rh-based catalysts depend on the reduction properties of the supports. CH_4 conversion was higher on Rh supported on unreducible oxides (Al_2O_3, MgO, Y_2O_3, La_2O_3, and SiO_2) than on reducible oxides (ZrO_2, CeO_2, and TiO_2), but no parallel measurements of Rh dispersion were reported. Even within the less

reducible supports, CH_4 conversions were sensitive to the identity of the support ($Rh/SiO_2 \approx Rh/Al_2O_3 \approx Rh/MgO > Rh/Y_2O_3 > Rh/La_2O_3$). Bhat and Sachtler [25] also found that CH_4 conversions during CO_2 reforming were sensitive to support effects ($Rh/Al_2O_3 > Rh/SiO_2 > Rh/NaZSM-5$). Neither study reported Rh dispersions or turnover rates. Thus, the observed support effects may simply arise from secondary effects of supports on Rh cluster size or on transport artifacts. In contrast, Mark and Maier [9] reported that the support (ZrO_2, Al_2O_3, TiO_2, SiO_2) did not influence CO_2 reforming turnover rates on Rh crystallites.

Here, we probe the identity and reversibility of elementary steps required for H_2O and CO_2 reforming of CH_4 on Rh of various dispersions on different supports (Al_2O_3 and ZrO_2). In doing so, we also establish a rigorous kinetic and mechanistic equivalence among water–gas shift, CH_4 decomposition, and CO_2 and H_2O reforming reactions. Kinetic and isotopic exchange measurement experiments confirmed the proposed catalytic sequence and the exclusive kinetic relevance of C–H bond activation steps and the kinetic irrelevance of co-reactant activation pathways on clean Rh surfaces. Transport artifacts were ruled out using bed and pellet dilution strategies, and measured rates were rigorously corrected for the distance from equilibrium in reforming reactions and for the number of exposed Rh surface atoms. Similar rate expressions and kinetic rate constants were measured for H_2O and CO_2 reforming and for CH_4 decomposition. Rate constants increased markedly with increasing Rh dispersion, but they did not depend on the identity of the support. These conclusions resemble those reached in parallel studies of CH_4 reforming and decomposition reactions on supported Ru, Ni, Ir, Pt, and Pd catalysts, the evidence for which will be presented elsewhere [29,35].

2. Experimental methods

2.1. Catalyst synthesis and characterization

Rh/Al_2O_3 and Rh/ZrO_2 catalysts with varying Rh content (0.1, 0.2, 0.4, 0.8, 1.6 wt%) were prepared by incipient wetness impregnation of Al_2O_3 or ZrO_2 with an aqueous solution of $Rh(NH_4)_3Cl_6$ (Alfa, CAS 10294-41-4, 99.99%) and dried at 393 K in ambient air for 12 h. These samples were then treated in flowing dry air (Airgas, UHP, 1.2 $cm^3/(g\,s)$) by increasing the temperature to 923 K at 0.167 $K\,s^{-1}$ and holding at 923 K for 5 h. A portion of each of the Rh/Al_2O_3 samples was treated in flowing dry air (Airgas, UHP, 1.2 $cm^3/(g\,s)$) at higher temperatures by increasing the temperature to 1123 K at 0.167 $K\,s^{-1}$ and holding at 1123 K for 5 h to achieve lower Rh dispersions. All samples were ultimately treated in pure H_2 (Airgas, UHP, 50 $cm^3/(g\,s)$) by heating to 973 K at 0.167 $K\,s^{-1}$ and holding at 973 K for 3 h before catalytic and chemisorption measurements. Al_2O_3 (160 m^2/g) was prepared by treating $Al(OH)_3$ (Aldrich, 21645-51-2) in flowing dry air (Airgas, UHP, 1.2 $cm^3/(g\,s)$)

while increasing the temperature to 923 K at 0.167 K s^{-1} and holding at 923 K for 5 h; this procedure led to γ-Al$_2$O$_3$ [36]. ZrO$_2$ (45 m^2/g) was prepared using procedures reported elsewhere [37], which led to the predominant formation of the monoclinic phase of ZrO$_2$ [37].

Rh dispersion was measured from volumetric H$_2$ chemisorption uptakes at 313 K using a Quantasorb chemisorption analyzer (Quantachrome Corp.). Samples were reduced in H$_2$ at 973 K for 2 h and then evacuated at 973 K for 0.5 h before chemisorption measurements. After cooling to 313 K, a H$_2$ chemisorption isotherm was measured at 3–50 kPa H$_2$. A backsorption isotherm was also measured after samples were evacuated at 313 K for 0.5 h. Both isotherms were extrapolated to zero H$_2$ pressure and their difference was used to measure strongly chemisorbed hydrogen uptakes, from which Rh dispersions were obtained by assuming a 1:1 stoichiometry between adsorbed H atoms and Rh surface atoms [38].

2.2. Catalytic CO$_2$ and H$_2$O reforming and stoichiometric decomposition of CH$_4$ on Rh crystallites

Catalytic rates were measured by placing samples (5 mg, 250–425 μm) in a quartz or stainless steel tube (8-mm inner diameter) equipped with a type *K* thermocouple enclosed within a sheath in contact with the catalyst bed. Samples were diluted with ground acid-washed quartz powder (500 mg, 250–425 μm) to avoid temperature gradients. Transport artifacts were ruled out using pellet and bed dilution tests, which led to undetectable variations in CH$_4$ reaction rates or selectivities. Kinetic effects of CH$_4$, H$_2$O, and CO$_2$ pressures on CH$_4$ reaction rates were measured at 823–1023 K and 100–1500 kPa total pressures over a wide range of reactant concentrations. Reactant mixtures were prepared using certified mixtures of 50% CH$_4$/Ar (Matheson, UHP) and 50% CO$_2$/Ar (Matheson, UHP) with He (Airgas, UHP) as balance. Deionized H$_2$O was introduced using a syringe pump (Cole-Parmer, 74900 series) for H$_2$O reforming reactions. All transfer lines were kept above 373 K after the point of H$_2$O introduction to avoid condensation. Reactant and product concentrations were measured with a Hewlett–Packard 6890 gas chromatograph using a Carboxen 1000 packed column (3.2 mm × 2 m) and a thermal conductivity detector.

Rh/Al$_2$O$_3$ (0.4 or 1.6 wt%, 20 mg, treated at 1123 K in air before reduction) diluted with 500 mg quartz powder was used in CH$_4$ and CD$_4$ decomposition kinetic measurements at 873 K. Chemical and isotopic compositions were measured by online mass spectrometry (Leybold Inficon, Transpector Series). Reactant mixtures with 20% CH$_4$/Ar or 20% CD$_4$/Ar were prepared using 50% CH$_4$/Ar (Matheson, certified mixture) or CD$_4$ (Isotec, chemical purity > 99.0%) and Ar (Airgas, UHP). Ar was used as an inert internal standard to measure CH$_4$ conversion. Initial CH$_4$ decomposition rates were used to estimate rate constants for CH$_4$ decompo-

sition based on the observed linear dependence of rates on CH$_4$ concentration.

2.3. Isotopic exchange and tracer measurements

Isotopic tracer studies were carried out on 0.1 wt% Rh/Al$_2$O$_3$ (treated in air at 1123 K before reduction) using a transient flow apparatus with short hydrodynamic delays (< 5 s). Chemical and isotopic compositions were measured by online mass spectrometry (Leybold Inficon, Transpector Series). CD$_4$ (Isotec, chemical purity > 99.0%), D$_2$O (Isotec, chemical purity > 99.0%), and 5% D$_2$/Ar and ^{13}CO (Isotec, chemical purity > 99.0%) were used as reactants without further purification. Intensities at 15 and 17–20 amu were used to measure methane isotopomer concentrations. CH$_4$ and CD$_4$ standard fragmentation patterns were measured and those for CHD$_3$, CH$_2$D$_2$, and CH$_3$D were calculated using reported methods [39]. Intensities at 17, 19, and 20 amu were used to determine water deutero isotopomers and those at 28, 29, 44, and 45 amu to measure ^{12}CO, ^{13}CO, ^{12}CO$_2$, and ^{13}CO$_2$ concentrations, respectively. Detailed experimental conditions are shown with the corresponding data in the results presented below.

2.4. Carbon formation measurement

Carbon formation rates were measured during reforming reactions at 873 K using a tapered-element quartz oscillating microbalance (Rupprecht & Patashnick, TEOM Series 1500 pma kinetic analyzer). Catalyst treatment procedures and reaction conditions were identical to those used in kinetic measurements.

2.5. CO oxidation rates

Structure-insensitive CO oxidation reactions were used to detect any changes in the number of exposed Rh atoms during CH$_4$ reforming. Rh/ZrO$_2$ (0.8 wt%, 10 mg; 500 mg quartz powder) was used to measure CO oxidation rates at 363 K and 0.19 kPa CO and 0.19 kPa O$_2$ pressures before and after CH$_4$ reforming reactions. Reactant and product concentrations were measured by gas chromatography using the protocols described above for CH$_4$ reactions. Mixtures of 25% O$_2$/He (Matheson, certified mixture) and 81.5% CO/N$_2$ (Matheson, certified mixture) were used as reactants.

3. Results and discussion

3.1. Kinetic dependence of forward CH$_4$ reaction rate on partial pressures of reactants and products

The kinetic dependencies of CH$_4$ reforming rates on CH$_4$, CO$_2$, and H$_2$O concentrations were similar on Rh/Al$_2$O$_3$ and Rh/ZrO$_2$ catalysts with different Rh contents. We report here detailed kinetic data only on a 0.4 wt% Rh/Al$_2$O$_3$ sample treated at 1123 K. Rates were measured under reaction con-

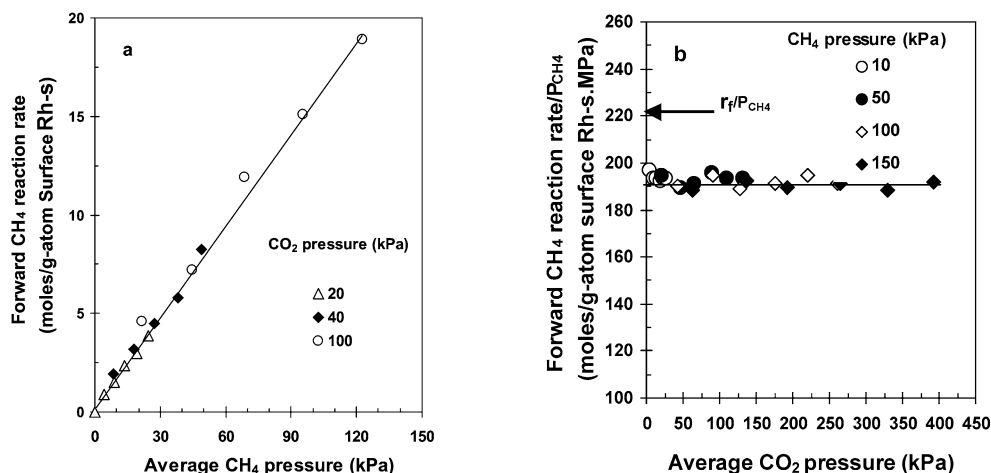Fig. 1. Effect of CH_4 (a) and CO_2 (b) partial pressure on forward CH_4 reaction rate for CO_2 reforming of CH_4 on 0.4 wt% Rh/Al_2O_3 treated at 1123 K (37.2% Rh dispersion) (5 mg catalyst, 873 K, total flow rate 100 cm^3/min, balance He).
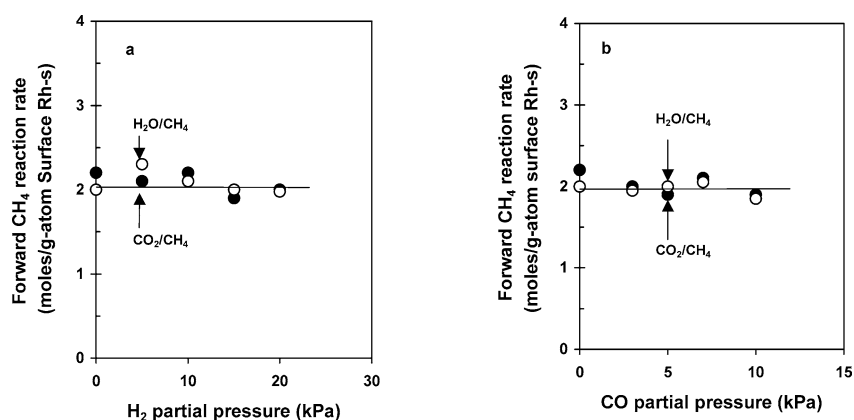

Fig. 2. Effect of H_2 (a) and CO (b) partial pressures on forward CH_4 reaction rate for CH_4 reforming reactions on 1.6 wt% Rh/Al_2O_3 treated at 1123 K (25.1% Rh dispersion) (873 K, 20 kPa CH_4, 20 kPa CO_2 or H_2O, 100 kPa total pressure, balance He).

ditions that led to stable rates without detectable carbon formation. The absence of filamentous carbon was confirmed by lack of detectable changes in the mass of samples during parallel microbalance measurements and by the lack of visual evidence for carbon filaments in transmission electron micrographs of samples used in catalytic reactions for extended periods of time.

Fig. 1 shows the effects of CH_4 and CO_2 pressures on forward CH_4 turnover rate (r_f) at 873 K and 100–1500 kPa total pressures; these turnover rates are normalized by the number of exposed surface Rh atoms measured by H_2 chemisorption uptakes before catalytic measurements. Measured net rates were corrected for the approach to equilibrium for each CH_4 reaction in order to obtain rigorous forward reaction rates. Specifically, measured rates were corrected for approach to equilibrium (η) from thermodynamic data [40] and the prevalent pressures of reactants and products using

$$\eta_2 = \frac{[P_{CO}]^2[P_{H_2}]^2}{[P_{CH_4}][P_{H_2O}]^2} \frac{1}{K_{EQ_2}}, \tag{2}$$

$$\eta_2 = \frac{[P_{CO}][P_{H_2}]^3}{[P_{CH_4}][P_{H_2O}]} \frac{1}{K_{EQ_2}} \tag{3}$$

for CH_4–CO_2 and CH_4–H_2O reactions, respectively. Here, $[P_j]$ is the average partial pressure of species j (in atm) and K_{EQ_1} and K_{EQ_2} are equilibrium constants at a given temperature [40]. Values of η range from 0 to 0.3 for experimental data reported here. Measured net reaction rates (r_n) are used to obtain forward rates (r_f) using [41]

$$r_n = r_f(1 - \eta). \tag{4}$$

This equation accurately describes all observed effects of reactor residence time and conversion on measured reaction rates.

Forward CO_2 reforming reaction rates increased linearly with increasing CH_4 partial pressures (5–450 kPa) at temperatures between 823 and 1023 K; these rates were not influenced, however, by CO_2 partial pressures (5–450 kPa) (Fig. 1). Fig. 2 shows that the addition of CO or H_2 to CH_4–CO_2 and CH_4–H_2O mixtures did not influence forward rates on 1.6 wt% Rh/Al_2O_3 (treated at 1123 K, 25.1% Rh dispersion) at 873 K. Forward rates were not influenced by CO or H_2 concentrations, whether they were varied by external addition or by changes in residence time and CH_4 conversion. Once additional effects of product concentrations on η are
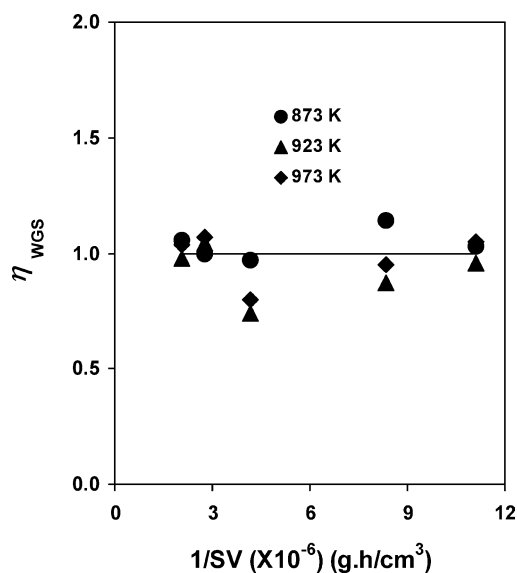
Fig. 3. Extent of water–gas shift equilibrium on Rh/Al_2O_3 at different reaction temperatures as a function of space velocity on 0.4 wt%-catalysts treated at 1123 K (37.2% Rh dispersion) (25 kPa CH_4, 25 kPa CO_2, 100 kPa total pressure, $\eta_{WGS} = ([P_{CO}][P_{H_2O}])/([P_{H_2}][P_{CO_2}]K_{WGS})$).

taken into account using Eqs. (2)–(4), CH_4 reforming rates using CO_2 as co-reactants become simply first-order in CH_4 and zero-order in CO_2,

$$r_f = k_{CO_2} P_{CH_4}. \tag{5}$$

The absence of co-reactant and product concentration effects indicates that the state of Rh surfaces is unaffected by the rate at which the products of CH_4 activation are removed by kinetic coupling of CH_4 activation steps with those required for co-reactant activation. These data also indicate that co-adsorbed products do not detectably influence the number of surface Rh atoms available for CH_4 activation steps. Castner et al. [42] have shown that H atoms recom-

bine and desorb from Rh(111) surfaces at 423–493 K, while CO desorbs at 498–548 K; thus, chemisorbed hydrogen and CO coverages are expected to be negligible at typical CH_4 reforming temperatures (873–1100 K).

Fig. 3 shows the extent of water–gas shift equilibrium under different reaction conditions on 0.4 wt% Rh/Al_2O_3. Measured concentrations of reactants and products during CH_4 reforming reactions showed that water–gas shift (WGS) reactions are equilibrated during CH_4 reforming on all Rh catalysts at 873–973 K. The more complex rate expressions reported in the literature appear to reflect transport artifacts or nonrigorous corrections for approach to thermodynamic equilibrium [16]. Our simple expression is consistent with CH_4 activation as the sole kinetically relevant elementary step and with fast and kinetically irrelevant reactions of CO_2 with CH_4-derived chemisorbed carbon to form CO; these fast steps maintain Rh surfaces essentially uncovered by adsorbed reactive intermediates during CH_4–CO_2 reactions.

The kinetic irrelevance of carbon removal by co-reactants was confirmed by the CH_4–H_2O reaction rates shown in Fig. 4. These rates are identical to those measured for CH_4–CO_2 mixtures at similar CH_4 partial pressures. As in the case of CO_2 reforming, forward CH_4 reaction rates using H_2O as the co-reactant depend linearly on the CH_4 partial pressure (5–25 kPa), but they are independent of the H_2O partial pressure (5–25 kPa); thus, the rate expression is identical to that for reactions of CH_4 with CO_2,

$$r_f = k_{H_2O} P_{CH_4}. \tag{6}$$

Moreover, the rate constants for H_2O (k_{H_2O}) and CO_2 (k_{CO_2}) reactions with CH_4 are identical within our experimental accuracy at each reaction temperature (Fig. 5). Activation energies are also similar for these two reaction mixtures (Table 1).

Rate constants measured during CH_4 reactions with CO_2 and H_2O co-reactants are also similar to those measured
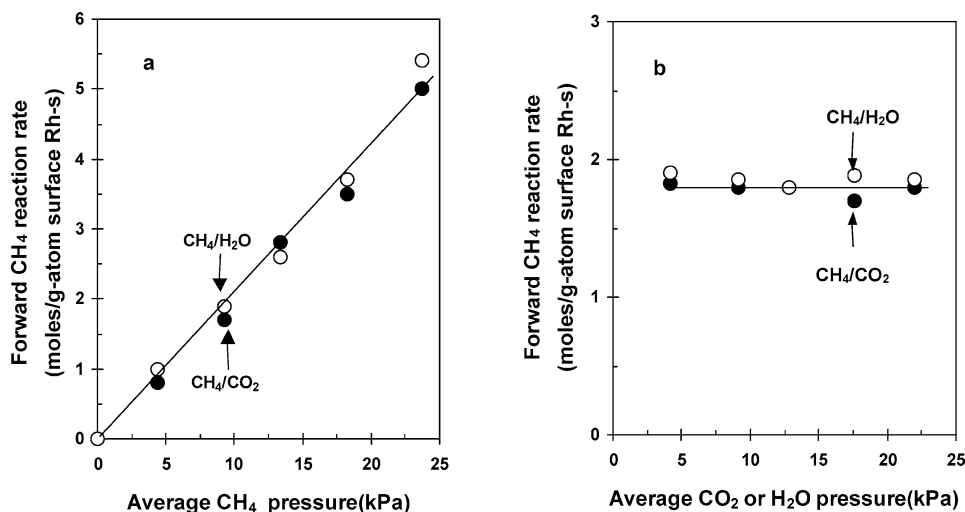
Fig. 4. Effect of CH_4 (a) and CO_2 or H_2O (b) partial pressure on forward CH_4 reaction rate for CH_4–CO_2 and CH_4–H_2O reactions on 0.4 wt% Rh/Al_2O_3 treated at 1123 K (37.2% Rh dispersion) (5 mg catalyst, 873 K, total flow rate 100 cm^3/min, 20 kPa CO_2 or H_2O in (a) and 10 kPa CH_4 in (b), 100 kPa total pressure, balance He).

Table 1
Forward CH_4 reaction rates, rate constants, activation energies, and preexponential factors for CH_4 reactions on 0.4 wt% Rh/Al_2O_3 calcined at 1123 K (37.2% Rh dispersion) (873 K, 20 kPa CH_4, 25 kPa CO_2 or H_2O, 100 kPa total pressure, balance Ar)

Co-reactant	Turnover rate[a] (s^{-1})	Rate constant $(s^{-1} kPa^{-1})$	Activation energy (kJ/mol)	Preexponential factor $(s^{-1} kPa^{-1})$	
				Measured	Estimated[b]
CO_2	4.2	0.21	111	9.2×10^5	5.5×10^3
H_2O	4.1	0.22	109	7.3×10^5	5.5×10^3
None	3.9	0.19	108	5.5×10^5	5.5×10^3

[a] Initial CH_4 turnover rate on Rh surface.
[b] Calculated based on transition-state theory treatments of CH_4 activation steps proceeding via an immobile activated complex [45].
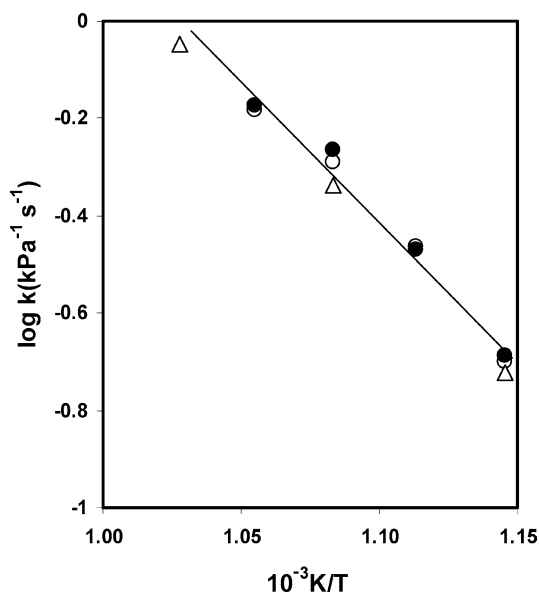

Fig. 5. Arrhenius plots for CO_2 reforming (●), H_2O reforming (○), and CH_4 decomposition (△) rate constants on 0.4 wt% Rh/Al_2O_3 treated at 1123 K (37.2% Rh dispersion).
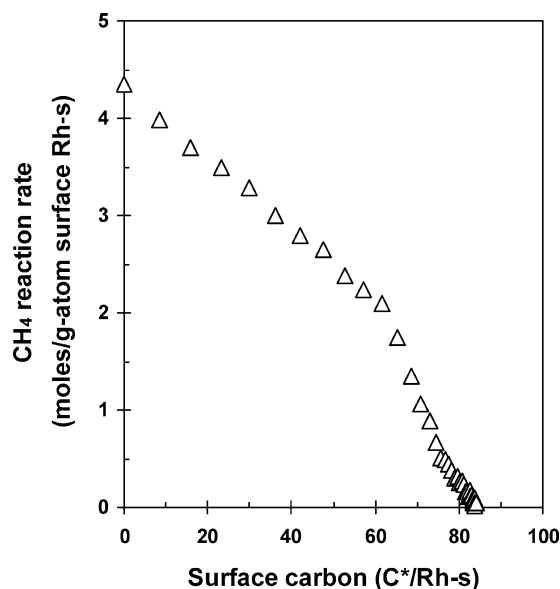

Fig. 6. CH_4 reaction rate for CH_4 decomposition on 0.4 wt% Rh/Al_2O_3 catalyst treated at 1123 K (37.2% Rh dispersion) (873 K, 25 kPa CH_4, 100 kPa total pressure, balance Ar).

in the absence of a co-reactant during the initial stages of CH_4 decomposition on 0.4 wt% Rh/Al_2O_3 (Fig. 6, Table 1). Clearly, the sole kinetically relevant step in catalytic reactions of CH_4 with H_2O or CO_2 to form H_2–CO mixtures and in stoichiometric decomposition of CH_4 to form C* and H_2 is the initial activation of a C–H bond in CH_4 catalyzed by interactions with surface Rh atoms. Also, the initial state of Rh surfaces during CH_4 decomposition and that during steady-state CH_4 reactions with H_2O or CO_2 are remarkably similar, suggesting the substantial absence of reactive or unreactive co-adsorbed species during steady-state catalysis.

The activation energies reported here (Table 1) agree with values previously reported for CO_2 reforming on 0.5 wt% Rh/Al_2O_3 (94.5 kJ/mol) [13], 1.0 wt% Rh/Al_2O_3 (88 kJ/mol) [23], 3.8 wt% Rh/SiO_2 (88 kJ/mol) [19], and 0.5 wt% Rh/Al_2O_3 (102 kJ/mol) [16]. In contrast, activation energies reported for dissociative adsorption of CH_4 on Rh films are significantly lower [43,44]. CH_4 dissociative adsorption on Rh films was reported to occur with an activation energy of only 29 kJ/mol [43] using field emission and molecular beam methods. Brass and Ehrlich [44] measured thermally averaged dissociation probabilities for CH_4 mole-

cular beams on Rh films and reported an activation energy of 46.4 kJ/mol. Density functional theory calculations gave C–H activation energies of 67, 32, and 20 kJ/mol for CH_4 reactions on flat Rh(111), stepped Rh(211), and kinked Rh surfaces, respectively [33]. These theoretical estimates for stepped and kinked Rh surfaces resemble those measured in molecular beam experiments on Rh films [43,44], but they are much lower than those for catalytic CO_2 and H_2O reforming on supported Rh clusters, even though C–H bond activation steps are the sole kinetically relevant step during steady-state catalysis.

The underlying reasons for these differences remain unclear, but they raise concerns about the fidelity and relevance of clean flat surfaces as models of working metal clusters during catalysis for both molecular beam experiments and theoretical calculations. It is possible that unreactive carbon deposits form via stoichiometric CH_4 reactions at coordinatively unsaturated edge or kink and steps on surfaces of small Rh clusters during catalytic CH_4 reactions with CO_2 or H_2O. This would occur as an intrinsic component of CH_4 activation pathways and as a natural consequence of the higher binding energy of such sites for C*, which also renders such

sites more effective than those on flatter surfaces at stabilizing transition states required for C–H bond activation. Such carbon species must be entirely unreactive during CH_4 reforming reactions because otherwise their surface density (and consequently the reaction rates) would vary with the concentration and identity of the co-reactant, leading to higher CH_4 reaction rates as the concentration or reactivity of co-reactants increases. These considerations make it unlikely that intrinsic surface passivation events are responsible for the observed discrepancies among various experimental and theoretical findings, because the expected wide range of reactivity for chemisorbed carbon species would make a significant subset of these species reactive toward CO_2 or H_2O as their respective concentrations increase during catalytic CH_4 reactions.

Preexponential factors for CH_4 activation during CH_4–CO_2 and CH_4–H_2O reactions are shown in Table 1, where values calculated using transition-state theory and immobile activated complexes [45] are also included for comparison. Measured preexponential factors are ~ 100 times larger than predicted for immobile activated complexes, indicating that the entropy of such activated complexes is significantly higher than expected from immobile species and that some two-dimensional translation occurs in the timescale of C–H bond activation events. We note that significant coverages of Rh surface atoms by unreactive carbon species would lead to lower than predicted preexponential factors. We also point out that using the low activation energies obtained in molecular beam and theoretical studies together with our measured catalytic turnover rates leads to absurdly large preexponential factors.

3.2. Dispersion and support effects on turnover rates for CH_4 reactions

Supported catalysts with a wide range of Rh dispersions (25.1–69.0%) and Rh crystallite diameters (1.4–4.0 nm) were prepared by varying the Rh content (0.1–1.6 wt%) and the thermal treatment temperature (923–1123 K) on Al_2O_3 and ZrO_2 supports. Rh dispersion decreased with increasing Rh content and treatment temperature, as expected from the greater sintering tendency of metal particles in both cases.

The effects of Rh dispersion and support identity on turnover rates (normalized by Rh surface atoms measured by H_2 chemisorption) for forward CO_2 and H_2O reactions with CH_4 are shown in Figs. 7a and 7b, respectively. Turnover rates and the effects of dispersion and support were identical for both reactions and also during the initial stages of CH_4 decomposition on Rh clusters without the presence of a co-reactant (Table 2), as expected from the rigorous kinetic and mechanistic equivalence among these three reactants.

Turnover rates increased monotonically with increasing Rh dispersion, suggesting that coordinatively unsaturated Rh surface atoms, prevalent in small clusters, are more active than those in low-index surface planes predominantly exposed on larger Rh crystallites. Edge and corner atoms, with

Table 2
Forward CH_4 turnover rates on Rh/Al_2O_3 catalysts treated at 1123 K (873 K, 20 kPa CH_4, 25 kPa CO_2 or H_2O, 100 kPa total pressure, balance Ar)

Rh load (%)	Rh dispersion (%)	Forward CH_4 turnover rate (s^{-1})		
		CH_4–CO_2	CH_4–H_2O	CH_4 decomposition
0.1	50.1	6.1	5.7	–
0.2	43.4	5.1	5.2	–
0.4	37.2	4.2	4.1	3.9
0.8	30.1	3.3	3.0	–
1.6	25.1	2.4	2.2	2.4

fewer Rh neighbors than those on terraces, appear to bind CH_x and H more strongly and to decrease the energy required to form relevant transition states for the initial C–H bond activation step [33]. Activation barriers from theoretical estimates were about 30 kJ/mol lower on stepped Rh(211) surfaces than on close-packed Rh(111) surfaces [33], although both are much lower than our experimental values, as discussed earlier. These surface roughness effects have also been reported for CH_4 dissociation on other metal surfaces. For example, CH_4 dissociation barrier estimates on flat Pd(111) and stepped Pd surfaces gave values of 65 and 37 kJ/mol, respectively [33]. Measured thermally averaged CH_4 dissociation rates on Pd single crystals increased with increasing density of steps and kinks [32] and were 10–100 times higher on stepped Pd(679) than on hexagonal close-packed Pd(111) surfaces. Kinks and steps are also much more active than terrace sites for alkane dissociation reactions on Ir [46] and Pt [47] surfaces. On supported Ni catalysts, CH_4 decomposition has been shown to occur faster on smaller Ni crystallites [48]. Zhang et al. [13] and Wang and Ruckenstein [17] reported that CH_4 turnover rates increased with increasing metal dispersion for CO_2–CH_4 reforming on Rh/Al_2O_3. These effects of surface structure and cluster size on CH_4 activation rates are consistent with the more extensive evidence for cluster size effects reported here for Rh supported on Al_2O_3 and ZrO_2. Taken together, these data confirm the structure sensitivity of C–H bond activation steps (by the definition of Boudart [34]) and their role as the sole kinetically relevant step in CO_2 or H_2O reforming of CH_4 and in CH_4 decomposition reactions.

The identity of the oxide surfaces on which Rh clusters are supported does not influence C–H bond activation steps or CH_4 conversion turnover rates, but it generally influences the size of Rh clusters for a given Rh content and thermal treatment protocol. When this Rh dispersion is used to obtain turnover rates, these turnover rates depend only on the size and structure of Rh clusters. Thus, it appears that electronic effects of the support on Rh clusters are weak in the size range of the clusters studied (1.4–4.0 nm) and that any involvement of the support in co-reactant activation, even if operative, is not kinetically relevant because overall reaction rates are limited only by C–H bond activation elementary steps, which are not catalyzed by the oxide supports. Some previous studies reported no detectable support

effects for CO_2 reforming of CH_4 on Rh [9,49] and Ir [9] catalysts, but others have observed significant effects, which have been used to implicate the support in co-reactant activation steps [50,51]. Tsipouriari et al. [50] reported that CH_4 turnover rates for CO_2 reforming are about two times greater on Rh/Al_2O_3 than on Rh/SiO_2, even though similar Rh dispersions of unity were claimed for both samples based on H_2 chemisorption. Nakamura et al. [51] proposed that CO_2 activation was the kinetically relevant step in $CO_2–CH_4$ reforming reactions on Rh and that Al_2O_3 supports increase the rate of CO_2 dissociation and thus overall reaction rates. Previous reports of support effects and of their involvement in co-reactant activation are inconsistent with the data presented in the current study and with the demonstrated kinetic irrelevance of co-reactant activation steps. Supports can influence metal dispersion and, in this manner, affect forward turnover rates, which are themselves very sensitive to the size of supported Rh clusters.

$CH_4–CO_2$ turnover rates on Rh-based catalysts reported by Zhang et al. [13] and Mark and Maier [9] are also shown in Fig. 7a. We have corrected these literature rates for approach to equilibrium and extrapolated to our reaction conditions (873 K, 20 kPa CH_4) using a first-order CH_4 dependence and the activation energy reported in the literature (94.5 kJ/mol [13]). The net rates reported in the literatures were assumed to be forward rates in view of the claimed differential conditions in these studies. Fig. 7a shows that these literature turnover rates for $CO_2–CH_4$ reactions and the data in the current study give consistent effects of dispersion, irrespective of the identity of the support.

Turnover rates reported here for CH_4 reforming are based on the number of exposed surface Rh atoms measured from H_2 chemisorption uptakes before reforming reactions. Sintering or blockage of Rh surfaces by unreactive chemisorbed species can occur and lead to Rh dispersions lower than those measured before reaction. We have used the oxidation

of CO, a structure–insensitive reaction [52,53], to probe the surface properties of working catalysts, because chemisorption measurements of used catalysts are not possible on the catalyst amounts (5 mg) used for steady-state CH_4 reforming reaction. These CO oxidation rate measurements are also helpful in ruling out artifacts in kinetic and activation energy estimates caused by effects of temperature or reactant concentrations on the extent of blockage or sintering. These effects, if present, may contribute to the significant differences in measured activation energies for CH_4 reforming on supported Rh catalysts [13,16,19] and for CH_4 activation on single crystals [43,44]. We note that the kinetic irrelevance of co-reactant activation steps indicates that any adsorbed species are unreactive during catalysis; thus any changes in Rh surface availability, as measured by CO oxidation, would indicate unreactive deposits or sintering.

CO oxidation and CH_4 reforming rates at 363 K on 0.8 wt% Rh/ZrO_2 are shown in Fig. 8. CO oxidation rates on fresh catalyst are similar to those measured after steady-state $CH_4–CO_2$ or $CH_4–H_2O$ reactions, indicating that exposed Rh atoms are not lost by sintering or covered by unreactive carbon residues during CH_4 reforming reactions. We cannot rigorously rule out that some Rh surface atoms ($< 5\%$) become unavailable during the first few turnovers and that such atoms exhibit uniquely reactive character for C–H bond activation. We can conclude, however, that such sites cannot turn over and are therefore catalytically inconsequential. These findings suggest that CH_4 chemistry on model surfaces must be extended beyond single-turnover stoichiometric activation reactions in both experimental and molecular simulations.

3.3. Isotopic evidence of kinetic relevance and reversibility of proposed elementary steps

In this section, we first present a hypothesis for a common mechanism for CO_2 and H_2O reforming and water–gas
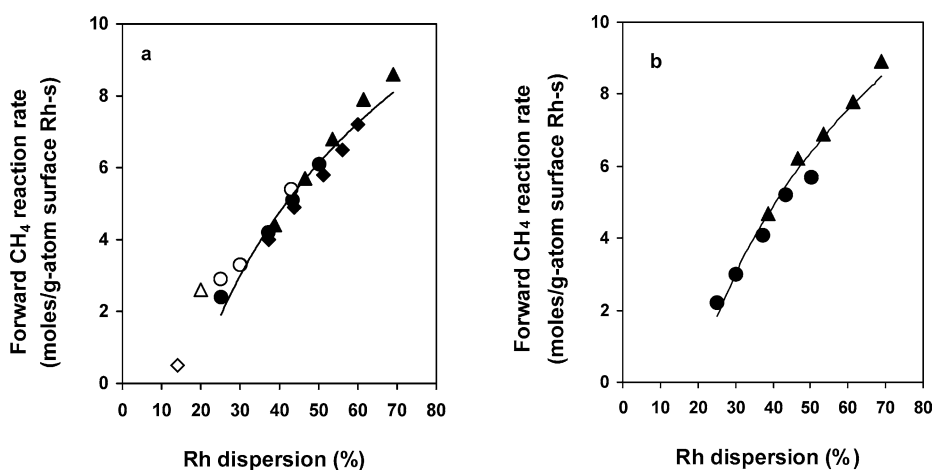

Fig. 7. Effects of Rh dispersion and support on forward CH_4 reaction rate for $CO_2–CH_4$ (a) and $CO_2–H_2O$ (b) reactions (873 K, 20 kPa CH_4, 20 kPa CO_2, 100 kPa total pressure, balance Ar. Solid symbols are the results of this study, and open symbols are from literature data. (●) Rh/Al_2O_3 treated at 1123 K (this study); (◆) Rh/Al_2O_3 treated at 923 K (this study); (▲) Rh/ZrO_2 treated at 923 K (this study); (◇) 5.0 wt% Rh/Al_2O_3 (Ref. [9]); (△) 0.5 wt% Rh/La_2O_3 (Ref. [13]); (○) Rh/Al_2O_3 (Ref. [13]).
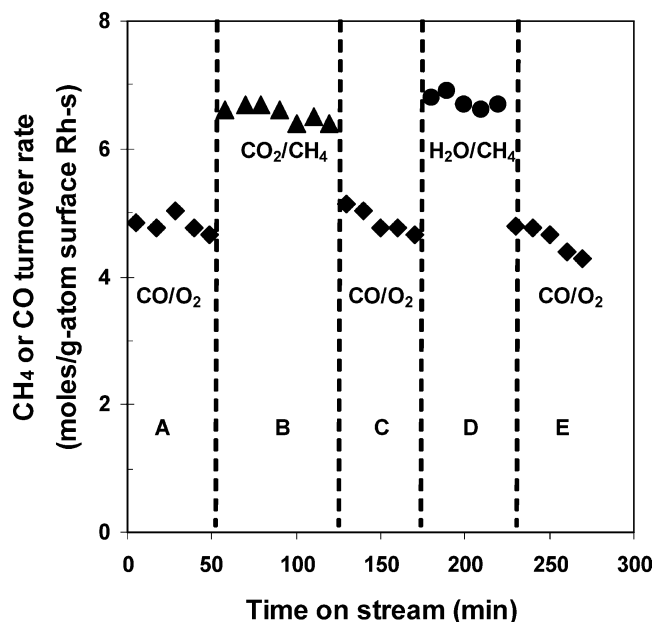
Fig. 8. CO oxidation and forward CH_4 reforming turnover rates on 0.8 wt% Rh/ZrO_2 (A, C, E, CO oxidation turnover rates, 363 K, 0.19 kPa CO, 0.19 kPa O_2; B, CO_2 reforming turnover rates, 873 K, 25 kPa CH_4, 25 kPa CO_2; D, H_2O reforming turnover rates, 873 K, 25 kPa CH_4, 25 kPa H_2O).

shift reactions and place it within the context of more complex previous proposals. Then, we present the results of isotopic tracing and exchange studies and kinetic isotope effect measurements carried out to probe this mechanistic hypothesis for CO_2 and H_2O reactions with CH_4 on supported Rh catalysts. The kinetic dependence of forward CH_4 reaction rates on reactants and products led us to propose a set of elementary steps involving simple intermediates, including chemisorbed carbon (reactions (7)–(17)). CH_4 decomposes to C^* in a series of elementary H-abstraction steps, and rate constants for subsequent H-abstractions are greater than those for the initial C–H bond activation [54]; this cascade process leads to low CH_x^* coverages and to C^* as the most abundant carbon-containing reactive intermediate. These C–H bond activation steps are followed by C^* and H^* removal via either desorption or reaction with chemisorbed O^* derived from CO_2 or H_2O co-reactants.

$$CH_4 + 2^* \xrightarrow{k_1} CH_3^* + H^*, \tag{7}$$

$$CH_3^* + ^* \longrightarrow CH_2^* + H^*, \tag{8}$$

$$CH_2^* + ^* \longrightarrow CH^* + H^*, \tag{9}$$

$$CH^* + ^* \longrightarrow C^* + H^*, \tag{10}$$

$$CO_2 + 2^* \xleftrightarrow{K_2} CO^* + O^*, \tag{11}$$

$$C^* + O^* \underset{k_{-3}}{\overset{k_3}{\rightleftarrows}} CO^{*} + ^*, \tag{12}$$

$$CO^* \xleftrightarrow{K_4} CO + ^*, \tag{13}$$

$$H^* + H^* \rightleftarrows H_2^* + ^*, \tag{14}$$

$$H^* + O^* \rightleftarrows OH^* + ^*, \tag{15}$$

$$OH^* + H^* \rightleftarrows H_2O^* + ^*, \tag{16}$$

$$H_2O^* \rightleftarrows H_2O + ^*. \tag{17}$$

Here, $\rightarrow$ denotes an irreversible step and $\rightleftarrows$ a quasi-equilibrated step, k_i is the rate coefficient, and K_i is the equilibrium constant for step i. When ($*$) is the most abundant surface intermediate, only the rate constant for step (7) appears in the rate expression and the overall CH_4 conversion rates become proportional to CH_4 concentration and independent of the identity or concentration of (CO_2 or H_2O) co-reactants. In these pathways, steps (11) and (13)–(17) are assumed to be reversible and quasi-equilibrated. We note that these elementary steps provide required pathways to complete CH_4 turnovers using either CO_2 or H_2O, but also a complete mechanism for water–gas shift reactions. Thus, this mechanism provides a unifying kinetic treatment for chemical reactions that are typically, but inappropriately and nonrigorously, treated as independent kinetic processes [15,16]. Mark and Maier [9] and Lercher et al. [55] proposed a similar reaction scheme on Rh- and Pt-based catalysts, respectively, without direct evidence or rigorous kinetic treatment, and they did not extend the sequence to include H_2O reforming or water–gas shift reactions.

The mechanism for CH_4 reactions with CO_2 (or H_2O) remains controversial and previous studies have reached contradictory conclusions. Efstathiou et al. [56] used isotopic switching experiments to conclude that carbon-containing species derived from CO_2 accumulated during CO_2 reforming on Rh/Al_2O_3, and proposed the elementary step

$$OH^* + C^* \longrightarrow CO^* + H^*. \tag{18}$$

We note that the kinetic relevance of this step would require significant differences between the rates of CH_4 conversion with CO_2 and H_2O co-reactants, in contradiction with the data presented here. This study concluded that CO_2 dissociation (step (11)) is the kinetically relevant step. CO_2 and CH_4 activation studies on Rh/Al_2O_3 led to the proposal that CH_4 dissociation occurs via reaction with chemisorbed oxygen (step (19)) formed via CO_2 dissociation, which was in turn aided by chemisorbed H atoms (step (20)) [49]:

$$CH_4^* + O^* \longrightarrow CH_3^* + OH^*, \tag{19}$$

$$CO_2^* + H^* \longrightarrow CO^* + OH^*. \tag{20}$$
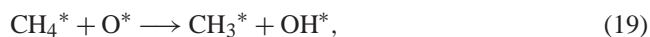
This proposal would lead to more complex pathways than in steps (7)–(17) and to reaction rates sensitive to the surface concentration of O^*, which would depend in turn on the reactivity and concentration of the co-reactants.

Kinetic isotope effects were measured from relative forward rates of CH_4–CO_2 and CD_4–CO_2 reactant mixtures at 873 K. For H_2O reforming, kinetic isotope effects were measured from forward reaction rates with CH_4–H_2O, CD_4–H_2O, and CD_4–D_2O mixtures at 873 K. Fig. 9 shows forward methane reaction rates for various isotopic reaction mixtures on 0.1 wt% Rh/Al_2O_3 (treated at 1123 K; 50.1% dispersion). Normal kinetic isotopic effects were measured
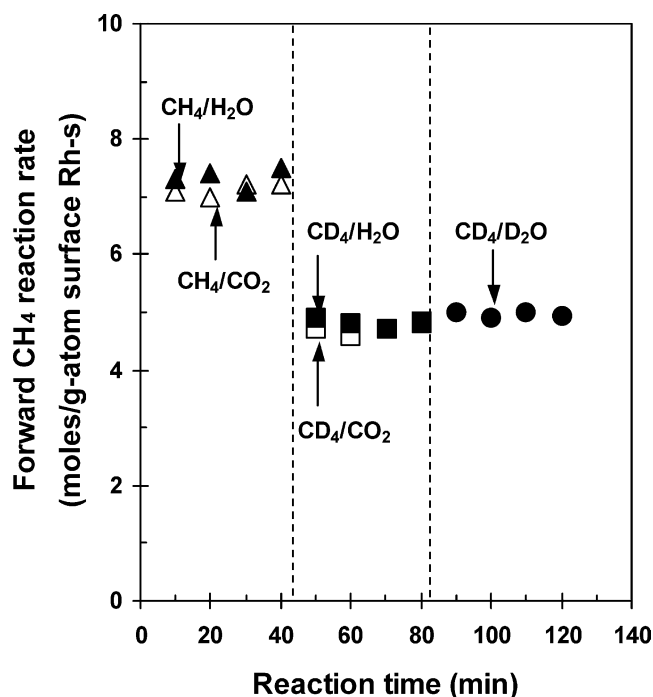
Fig. 9. Kinetic isotopic effects during the exchanges of CH_4/CO_2 ($\triangle$) $\rightarrow$ CD_4/CO_2 ($\square$) and CH_4/H_2O ($\blacktriangle$) $\rightarrow$ CD_4/H_2O ($\blacksquare$) $\rightarrow$ CD_4/D_2O ($\bullet$) on 0.1 wt% Rh/Al$_2$O$_3$ (5 mg catalyst, 873 K, 25 kPa CO$_2$ or H$_2$O, 25 kPa CH$_4$ or CD$_4$, 100 kPa total pressure, balance Ar).

Table 3
Kinetic isotope effects for CH$_4$ reactions on Rh/Al$_2$O$_3$ (873 K, 25 kPa CH$_4$ or CD$_4$, 25 kPa CO$_2$ or H$_2$O, 100 kPa total pressure, balance Ar)

Co-reactants	CO_2	H_2O	None
k_{CH_4}/k_{CD_4}	1.56	1.54	1.60

Table 4
Methane reaction rate and CH$_4$/CD$_4$ cross-exchange rates during the reaction of CH$_4$/CD$_4$/CO$_2$ mixture on 0.1 wt% Rh/Al$_2$O$_3$ catalyst (873 K, 12.5 kPa CH$_4$ and CD$_4$, 25 kPa CO$_2$, 100 kPa total pressure, balance Ar)

Methane turn-over rate (s^{-1})[a]	Cross exchange rate (s^{-1})[b]			$r_{exch}/r_{reaction}$[c]	η[d]
	CHD$_3$	CH$_2$D$_2$	CH$_3$D		
6.10	0.09	0.08	0.07	0.04	0.03

[a] Forward methane chemical conversion rate.
[b] Methane isotopomer formation rate.
[c] The ratio of total methane isotopomers formation rate to the methane chemical conversion rate.
[d] $\eta = ([P_{CO}]^2[P_{H_2}]^2)/([P_{CO_2}][P_{CH_4}]K)$.

for both CH$_4$–CO$_2$ (1.56) and CH$_4$–H$_2$O (1.54) reactions and also for CH$_4$ decomposition (1.60) (Table 3); their values are the same within our experimental accuracy (1.54–1.60). This normal kinetic isotopic effect for CH$_4$ activation is consistent with kinetically relevant C–H bond activation steps (step (7)). Replacing H$_2$O with D$_2$O did not influence steam reforming rates (Fig. 9), indicating that steps involving water activation, reaction of C* with hydroxyl groups, and hydrogen desorption are not kinetically relevant. Elmasides and Verykios [57] measured a kinetic isotope value of 1.6 for partial oxidation of CH$_4$–O$_2$ reactant mixtures at 903 K on Ru/TiO$_2$. This value is very similar to those reported here for H$_2$O and CO$_2$ reforming reactions on Rh-based catalyst, suggesting that partial oxidation reactions may also involve C–H activation as the sole kinetically relevant elementary step.

The reversibility of C–H bond activation steps was probed by measuring the rate of formation of CH$_{4-x}$D$_x$ isotopomers during reactions of CH$_4$/CD$_4$/CO$_2$ mixtures. Reversible C–H bond activation would lead to comparable rates of chemical conversion and cross-exchange, because the latter reflect the microscopic reverse of C–H bond activation steps. Irreversible steps would lead instead to cross-

exchange rates much lower than chemical conversion rates. The reaction of CH$_4$/CD$_4$/CO$_2$ (1:1:2) mixture was carried out at 873 K on 0.1 wt% Rh/Al$_2$O$_3$; chemical conversion and isotopic exchange rates were measured by online mass spectrometry, after removal of H$_x$D$_{2-x}$O by cooling the effluent to 218 K. Rates of CH$_{4-x}$D$_x$ ($0 < x < 4$) formation and of methane chemical conversion are shown in Table 4. CH$_4$/CD$_4$ cross-exchange rates (0.24 s^{-1}) are much lower than chemical conversion rates (6.1 s^{-1}), indicating that C–H bond activation is essentially irreversible; the microscopic reverse of C–H activation occurs, on average, once every 25 chemical conversion turnovers. The approach to equilibrium for CO$_2$ reforming, η, was 0.03 in this experiment; thus, C–H bond activation steps are as reversible as the overall chemical reaction, a condition that must be satisfied by the sole kinetically relevant step in any reversible chemical reaction mechanism.

The H/D ratio in the hydrogen formed from these equimolar CH$_4$–CD$_4$ mixtures is higher than unity (1.78) and shows a binomial isotopomer distribution. This reflects the higher reactivity of CH$_4$ relative to CD$_4$; this ratio is very similar to the value of the kinetic isotope effect measured from independent CH$_4$–CO$_2$ and CD$_4$–CO$_2$ reactant mixtures. The binomial distribution of dihydrogen isotopomers provides indirect and preliminary evidence for the quasi-equilibrated nature of recombinative hydrogen desorption steps.

Water forms during CO$_2$ reforming of CH$_4$ because some elementary steps lead to the removal of O* formed via CO$_2$ dissociation by reaction with H* instead of C* in a manner that affects reversible water–gas shift reactions. The composition of the products formed suggests that these steps are at equilibrium during CO$_2$ reforming (Fig. 3). As a result, water formation must involve quasi-equilibrated elementary steps. CH$_4$/CO$_2$/D$_2$ (1:1:0.2) mixtures were reacted on 0.1 wt% Rh/Al$_2$O$_3$ at 873 K. No deuterated methane isotopomers were detected in the effluent, as expected from irreversible C–H bond activation and the low η values (< 0.05) in these experiments. The H/D fraction expected in water and dihydrogen if all H atoms in chemically converted CH$_4$ mixed rapidly with all D atoms in D$_2$ within a pool of surface intermediates is 0.70. Water and dihydrogen in the effluent contained H/D ratios of 0.69 and 0.71, respectively,
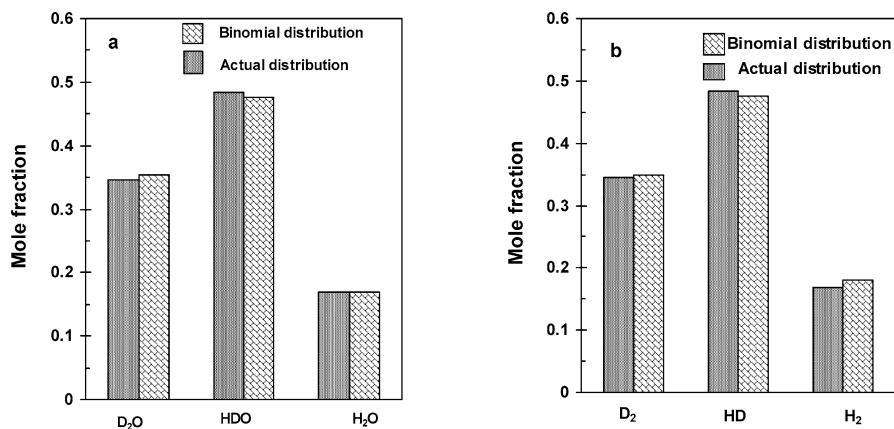
Fig. 10. Distribution of water (a) and dihydrogen (b) isotopomers during reactions of $CH_4/CO_2/D_2$ mixtures on 0.1 wt% Rh/Al_2O_3 treated at 1123 K (50.1% Rh dispersion) (873 K, 16.7 kPa CH_4, 16.7 kPa CO_2, 3.3 kPa D_2, 100 kPa total pressure, balance Ar).

indicating that complete equilibration occurs between dihydrogen and water gaseous species and their corresponding chemisorbed precursors and intermediates. Fig. 10a shows the binomial isotopomer distribution detected in the water formed from $CH_4/CO_2/D_2$ mixtures, consistent with fast and quasi-equilibrated recombination of H* and OH* (step (16)). Similar binomial distributions were observed for dihydrogen isotopomers (Fig. 10b), indicating that recombinative hydrogen desorption (step (14)) is also quasi-equilibrated during CH_4/CO_2 reactions on Rh/Al_2O_3 at 873 K.

The reversibility of CO_2 activation steps (step (11)) was probed using $^{12}CH_4/^{12}CO_2/^{13}CO$ (1:1:0.2) reactant mixtures on 0.1 wt% Rh/Al_2O_3 at 873 K. The ^{13}C fraction was similar in the CO (0.148) and CO_2 (0.138) present in the reactor effluent under conditions far from equilibrium ($\eta < 0.05$), even though reactant mixtures consisted of pure $^{12}CO_2$ and ^{13}CO. This ^{13}C content corresponds to complete chemical and isotopic equilibration between CO and CO_2, even at low CH_4 chemical conversions (3.5%). These data indicate that CO_2 dissociation steps are much faster than kinetically relevant CH_4 dissociation steps and that steps (11) and (13) take place (in both directions) many times in the time required for one CH_4 chemical conversion turnover. Thus, CO_2 activation steps are reversible and quasi-equilibrated during $CH_4–CO_2$ reactions and, by inference from the kinetic and mechanistic equivalence of $CH_4–CO_2$ and $CH_4–H_2O$ reactions, also during the latter reaction. $^{13}CH_4$ was not detected during reactions of $^{12}CH_4/^{12}CO_2/^{13}CO$ mixtures, because the overall reaction is far from equilibrium ($\eta < 0.05$) during these experiments.

Quasi-equilibrated steps leading to water and dihydrogen and to $CO–CO_2$ interconversion, taken together with the expected equilibration of fast CO adsorption–desorption steps, require that the water–gas shift reaction must also be quasi-equilibrated during $CH_4–CO_2$ and $CH_4–H_2O$ reactant mixtures on Rh catalysts, as indeed found (Fig. 3). In view of the kinetic equivalence of elementary steps involved in CH_4 reactions with CO_2 and H_2O, we consider these conclusions

to be rigorously applicable also to $CH_4–H_2O$ reactions on Rh-based catalysts.

CH_4 reforming pathways shown in steps (7)–(17) are consistent with rate and isotopic measurements using CO_2 and H_2O co-reactants, with the mechanistic equivalence of $CH_4–H_2O$ and $CH_4–CO_2$ reactions, and with the quasi-equilibrated nature of steps leading to water–gas shift. The first C–H bond activation step solely determines overall reaction rates and it is exactly as reversible as the overall CH_4 chemical reaction. Co-reactant activation is fast and quasi-equilibrated and leads to Rh surfaces that are essentially unaffected by the rate at which C* is removed by the co-reactant. Isotopic studies were carried out using 0.1 wt% Rh/Al_2O_3 and predominately at 873 K, but the similar rate expressions obtained at all temperatures and on all supported Rh catalysts indicate that these mechanistic conclusions are valid for Rh catalysts in general. Parallel studies of CH_4 reactions with H_2O and CO_2 on Ru [29], Ir, Pt, and Ni [35] have led to similar conclusions about the identity, reversibility, and kinetic relevance of the elementary steps in steps (7)–(17). We note that these elementary steps also provide a rigorous basis for kinetic treatments of carbon filament formation during CH_4 reforming reactions, as we discuss in detail elsewhere [35]. For these treatments, C* concentrations and the identity and reactivity of co-reactants become relevant for kinetic descriptions of carbon formation, even when these properties remain unimportant in determining kinetic rates of CH_4 chemical conversion to synthesis gas.

4. Conclusions

Forward rates and activation energies for CH_4 reforming turn over rates were identical with those for CO_2 and H_2O co-reactants and similar to values obtained during the initial stages of stoichiometric CH_4 decomposition on Rh clusters supported on Al_2O_3 and ZrO_2. Reaction rates were proportional to CH_4 pressures and independent of the identity and concentration of co-reactants. The concentration of

reaction products influenced net rates only by varying the distance from equilibrium for the overall reaction; their effects disappear when these thermodynamic effects are taken into account by converting experimental net rates to forward reaction rates. Measured kinetic isotope effects were also independent of co-reactant, and their values are consistent with the sole kinetic relevance of C–H bond activation steps and with fast scavenging of chemisorbed carbon intermediates by both H_2O and CO_2, which leads to Rh surfaces essentially free of adsorbed reaction intermediates. These conclusions are consistent with isotopic tracer studies, which indicate that H and OH species recombine rapidly to form H_2 or H_2O in quasi-equilibrated steps and that CO_2 and H_2O dissociations are also quasi-equilibrated during CH_4 reforming reactions. Turnover rates increased monotonically with increasing Rh dispersion for CH_4 reactions with CO_2 or H_2O and for CH_4 decomposition reactions, suggesting that coordinative unsaturation of surface Rh atoms leads to more stable transition states for CH_4 dissociation reactions. The identity of the support influenced Rh dispersions, but not CH_4 reforming turn over rates; any roles of supports in co-reactant activation cannot lead to detectable changes in CH_4 reforming turnover rates because co-reactant activation is not kinetically relevant.

Acknowledgments

References

[1] J.H. Edwards, A.M. Maitra, Fuel Processing Tech. 42 (1995) 269.
[2] S.B. Wang, G.Q. Lu, Energy Fuels 10 (1996) 896.
[3] M.C.J. Bradford, M.A. Vannice, Catal. Rev. Sci. Eng. 41 (1999) 1.
[4] V.F. Fischer, H. Tropsch, Brennstoff-Chemie 3 (1928) 39.
[5] J.R. Rostrup-Nielsen, J.H. Bak Hansen, J. Catal. 144 (1993) 38.
[6] J.H. Bitter, S. Seshan, J.A. Lercher, J. Catal. 176 (1998) 93.
[7] Y. Sakai, H. Saito, T. Sodesawa, F. Nozaki, React. Kinet. Catal. Lett. 24 (1984) 253.
[8] A.T. Ashcroft, A.K. Cheetham, M.L.H. Green, P.D.F. Vernon, Nature 352 (1991) 225.
[9] M.F. Mark, W.F. Maier, J. Catal. 164 (1996) 122.
[10] F. Solymosi, G. Kutsan, A. Erdohelyi, Catal. Lett. 11 (1991) 149.
[11] S. Yokota, K. Okumura, M. Niwa, Catal. Lett. 84 (2002) 131.
[12] U.L. Portugal, A.C.S.F. Santos, S. Damyanova, C.M.P. Marques, J.M.C. Bueno, J. Mol. Catal. A: Chem. 184 (2002) 311.
[13] Z.L. Zhang, V.A. Tsipouriari, A.M. Efstathiou, X.E. Verykios, J. Catal. 158 (1996) 51.
[14] L. Basini, D. Sanfilippo, J. Catal. 157 (1995) 162.
[15] M.F. Mark, F. Mark, W.F. Maier, Chem. Eng. Technol. 20 (1997) 361.
[16] J.T. Richardson, S.A. Paripatyadar, Appl. Catal. 61 (1990) 293.
[17] H.Y. Wang, E. Ruckenstein, Appl. Catal. 204 (2000) 143.
[18] H.Y. Wang, E. Ruckenstein, J. Phys. Chem. 103 (1999) 11327.
[19] M. Sigl, M.C.L. Bradford, H. Knozinger, M.A. Vannice, Topics in Catal. 8 (1999) 211.
[20] H.Y. Wang, C.T. Au, Appl. Catal. A 155 (1997) 239.
[21] P. Gronchi, P. Centola, R. Del Rosso, Appl. Catal. A 152 (1997) 83.
[22] D. Qin, J. Lapszewicz, Catal. Today 21 (1994) 551.
[23] J. Nakamura, K. Aikawa, K. Sato, T. Uchijima, Catal. Lett. 25 (1994) 265.
[24] M.C.J. Bradford, M.A. Vannice, Catal. Today 50 (1999) 87.
[25] R.N. Bhat, W.M.H. Sachtler, Appl. Catal. A 150 (1997) 279.
[26] F. Solymosi, A. Szoke, L. Ehri, Topics Catal. 8 (1999) 249.
[27] M.J. Hei, H.B. Chen, J. Yi, D.W. Liao, Surf. Sci. 417 (1998) 82.
[28] M.F. Mark, W.F. Maier, Angew. Chem. Int. Edit. 33 (1994) 1657.
[29] J. Wei, E. Iglesia, J. Phys. Chem. B, in press.
[30] R. Pitchai, K. Klier, Catal. Rev.-Sci. Eng. 28 (1986) 13.
[31] M.C. McMaster, R.J. Madix, J. Chem. Phys. 98 (1993) 15.
[32] K. Klier, J.S. Hess, R.G. Herman, J. Chem. Phys. 107 (1997) 4033.
[33] Z. Liu, P. Hu, J. Am. Chem. Soc. 125 (2003) 1958.
[34] M. Boudart, Adv. Catal. 20 (1969) 153.
[35] J. Wei, E. Iglesia, J. Catal. 224 (2004) 370.
[36] N. Bahlawane, T. Watanabe, J. Am. Ceram. Soc. 83 (2000) 2324.
[37] D.G. Barton, PhD dissertation, University of California at Berkeley, 1998.
[38] C. Force, A. Ruiz Paniego, J.M. Guil, J.M. Gatica, C. López-Cartes, S. Bernal, J. Sanz, Langmuir 17 (2001) 2720.
[39] G.L. Price, E. Iglesia, Ind. Eng. Chem. 28 (1989) 839.
[40] D.R. Stull, F. Edgar, J. Westrum, G.C. Sinke, The Thermodynamics of Organic Compounds, Krieger, Malabar, FL, 1987.
[41] M. Boudart, G. Djega-Mariadassou, The Kinetics of Heterogeneous Catalytic Reactions, Princeton University Press, Princeton, NJ, 1984.
[42] D.G. Castner, B.A. Sexton, G.A. Somorjai, Surf. Sci. 71 (1978) 519.
[43] C.N. Stewart, G. Ehrlich, J. Chem. Phys. 62 (1975) 4672.
[44] S.G. Brass, G. Ehrlich, J. Chem. Phys. 87 (1987) 4285.
[45] J.A. Dumesic, D.F. Rudd, J.E. Rekoske, A.A. Trevino, The Microkinetics of Heterogeneous Catalysis, American Chemical Society, Washington, DC, 1993.
[46] D.F. Johnson, W.H. Weinberg, J. Chem. Phys. 101 (1994) 6289.
[47] J.F. Weaver, M.A. Krzyzowski, R.J. Madix, Surf. Sci. 391 (1997) 150.
[48] E.G.M. Kuijpers, A.K. Breedijk, W.J.J. van der Wal, J.W. Geus, J. Catal. 81 (1983) 429.
[49] A. Erdöhelyi, J. Cresényi, F. Solymosi, J. Catal. 141 (1993) 287.
[50] V.A. Tsipouriari, A.M. Efstathiou, Z.L. Zhang, X.E. Verykios, Catal. Today 21 (1994) 579.
[51] K. Nakamura, K. Aikawa, K. Sato, T. Uchijima, Stud. Surf. Sci. Catal. 90 (1993) 95.
[52] M. Boudart, F.F. Rump, React. Kinet. Catal. Lett. 135 (1987) 95.
[53] G. Engel, G. Ertl, J. Chem. Phys. 69 (1978) 1267.
[54] C. Au, C. Ng, M. Liao, J. Catal. 185 (1999) 12.
[55] J.A. Lercher, J.H. Bitter, W. Hally, W. Niessen, K. Seshan, Stud. Surf. Sci. Catal. 101 (1996) 463.
[56] A.M. Efstathiou, A. Kladi, V.A. Tsipouriari, X.E. Verykios, J. Catal. 158 (1996) 64.
[57] C. Elmasides, X.E. Verykios, J. Catal. 203 (2001) 477.